Received: 13 April 2019 | Revised: 26 June 2019 | Accepted: 20 July 2019

DOI: 10.1002/aic.16737

PROCESS SYSTEMS ENGINEERING

AIChE JOURNAL

Global minimization of total exergy loss of multicomponent distillation configurations

Zheyu Jiang[1] | Zewei Chen[1] | Joshua Huff[1] | Anirudh A. Shenvi[1] | Mohit Tawarmalani[2] | Rakesh Agrawal[1]

[1]Davidson School of Chemical Engineering, Purdue University, West Lafayette, Indiana

[2]Krannert School of Management, Purdue University, West Lafayette, Indiana

Correspondence
Mohit Tawarmalani, Krannert School of Management, Purdue University, West Lafayette, IN 47907.
Email: mtawarma@purdue.edu;
and
Rakesh Agrawal, Davidson School of Chemical Engineering, Purdue University, West Lafayette, IN 47907.
Email: agrawalr@purdue.edu

Funding information
U.S. Department of Energy, Grant/Award Number: DE-EE0005768

Abstract

The operating cost of a multicomponent distillation system comprises two major aspects: the overall heat duty requirement and the temperature levels at which the heat duties are generated and rejected. The second aspect, often measured by the thermodynamic efficiency of the distillation system, can be quantified by its total exergy loss. In this article, we introduce a global optimization framework for determining the minimum total exergy loss required to distill any ideal or near-ideal multicomponent mixture using a sequence of columns. Desired configurations identified by this new framework tend to use milder-temperature reboilers and condensers and are thus attractive for applications such as heat pump assisted distillation. Through a case study of shale gas separations, we demonstrate the effectiveness of this framework and present various useful physical insights for designing energy efficient distillation systems.

KEYWORDS
distillation configuration, exergy analysis, global optimization, multicomponent distillation, thermodynamic efficiency

1 | INTRODUCTION

Distillation is an important separation process that accounts for most separations in chemical process industries.[1] It deals with some of world's largest and most profitable industrial separations, such as crude oil fractionation, hydrocarbon separations from steam cracking, and natural gas liquids (NGLs) separations. For separating a multicomponent mixture containing n components into its individual constituents, a sequence of distillation columns also known as a *distillation configuration* are generally needed. The most widely implemented group of configurations in practice uses exactly $n - 1$ distillation columns. We refer to this group of configurations as the *regular-column configurations*.[2] Regular-column configurations can be categorized as either *basic* or *thermally coupled*. In a basic configuration, each column is associated with one reboiler and one condenser.[3] But in a thermally coupled configuration, one or more intermediate reboilers and/or condensers associated with intercolumn submixture transfers (i.e., heat exchangers that do not produce final pure products) are replaced by two-way vapor–liquid communications known as thermal couplings. Regular-column configurations can also be classified as either *sharp split configurations* or *non-sharp split configurations*.[4] A split represents the separation of a mixture into two product streams. Sharp splits produce product streams with no overlapping components, whereas non-sharp splits produce product streams with a non-negligible amount of overlapping components. Sharp split configurations contain only sharp splits, and non-sharp split configurations contain one or more non-sharp splits.

The number of regular-column configurations increases combinatorially as the number of components in the feed increases.[5] As a result, the complete enumeration of the search space containing all regular-column configurations has been a challenge for decades. In an early approach, Thompson and King[6] provided a method to generate all sharp split configurations. Sargent and Gaminibandara[7] presented a superstructure framework to include both sharp and non-sharp split

configurations, but this framework did not cover all feasible configurations. Agrawal[8] then proposed a superstructure and discovered a new class of configurations with all columns other than the main feed column being placed around the main feed column in a satellite-like arrangement. However, the problem of complete enumeration of all regular-column configurations remained unsolved until Agrawal[3] proposed a rule-based enumeration approach, which laid the foundation for subsequent approaches by Caballero and Grossmann,[9] Ivakpour and Kasiri,[10] and finally, by Shah and Agrawal.[5] Specifically, Shah and Agrawal[5] developed a simple and elegant step-wise procedure, also known as the SA method,[11] to systematically enumerate the complete search space of all sharp and non-sharp split basic and thermally coupled regular-column configurations.

These regular-column configurations, although all performing the same separation task using the same number of distillation columns, can have very different capital and operating costs. In particular, the operating cost or energy consumption of a distillation configuration comprises two major aspects: the total reboiler heat duty requirement, which is proportional to the sum of vapor flows generated at all reboilers per unit time, as well as the temperature levels at which the heat duties are generated by the reboilers and rejected by the condensers.[12] The first aspect is associated with the first-law heat-duty demand of a distillation configuration, whereas the second aspect is closely related to the heating and cooling utility costs (second-law temperature-level costs) of the reboilers and condensers. Here, we clearly distinguish the difference between "energy" and "heat." Although most people have been primarily focusing on the absolute value of overall heat duty needed in a configuration, less attention has been paid on the temperature levels at which the generation and removal of heat duties occur, that is, the qualities of the heat duties. Failure to recognize and consider both aspects may lead to the design of inefficient distillation systems.[12,13]

Thermodynamic efficiency analysis is a useful tool to evaluate the energy performance of a multicomponent distillation system.[14,15] One of the classic industrial examples that illustrates the importance and potency of thermodynamic efficiency analysis is the separation of air into high purity nitrogen, oxygen, and argon products. This separation, which is conducted at cryogenic conditions, is primarily driven by *work* instead of *heat*. Thus, the thermodynamic efficiency of this process is characterized using the following definition:[16]

$$\eta = \frac{\text{minimum work of separation}}{\text{total work of separation}} \quad (1)$$

Under this definition of Equation (1), Agrawal and Fidkowski[12] based on an earlier important observation by Agrawal and Herron[17] that it was possible to derive thermodynamic efficiency expressions for binary separations without explicit knowledge of reboiler and condenser temperatures, extended the method to calculate the thermodynamic efficiency for each of the three ternary thermally coupled configurations shown in Figure 1. In this figure, and also in all subsequent figures, capital letters *A*, *B*, *C*, and so on represent pure components with their volatilities decreasing in alphabetical order. It is determined that the side-rectifier configuration of Figure 1b has the highest thermodynamic efficiency of 44.52%, which is consistent with the industrial practice for argon recovery that has been in use for over 85 years.[18] However, the three-component fully thermally coupled (FTC) Petlyuk configuration[19] of Figure 1c, which is known to always have the lowest total heat duty requirement among all configurations, has only 1/3 the thermodynamic efficiency of the side-rectifier configuration. This is because, although the FTC configuration requires the lowest possible heat duty, all the heat is generated at the highest temperature reboiler (i.e., reboiler at *C* of Figure 1c) and removed at the lowest temperature condenser (i.e., condenser at *A* of Figure 1c). Thus, it is not surprising that, in spite of many attempts trying to improve the energy efficiency of the FTC configuration,[20] it has not found any successful application in cryogenic air separation. In fact, for ternary separations, the range of feed conditions under which the FTC configuration has a higher thermodynamic efficiency than other configurations turns out to be quite limited.[12] Flores et al.[21] also reached similar conclusions when considering a set of cases involving ternary and quaternary separations.

The usefulness of thermodynamic efficiency analysis is not only limited to cryogenic separations but also in applications such as heat pump assisted distillation, multi-effect distillation, heat-integrated distillation, vapor recompression distillation, and so on. These applications may or may not have to be operated at subambient conditions.

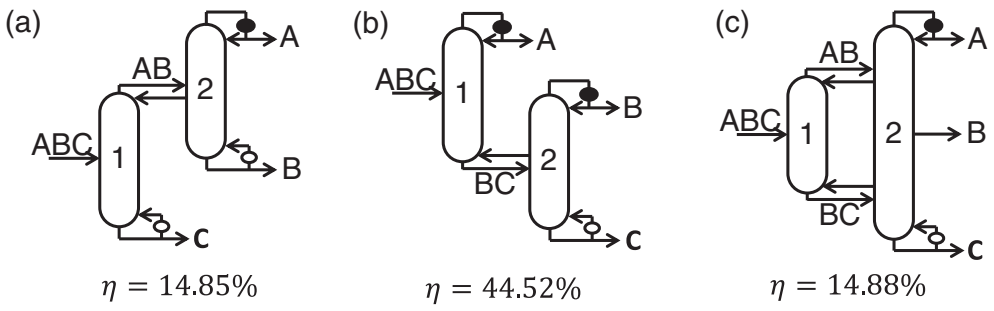

FIGURE 1 (a) Indirect split thermally coupled configuration, which is equivalent to the side-stripper scheme; (b) direct split thermally coupled configuration, which is equivalent to the side-rectifier scheme; (c) the fully thermally coupled (FTC) Petlyuk column.[19] The thermodynamic efficiencies for these configurations are determined by Agrawal and Fidkowski.[12] In this example, *A* = nitrogen, *B* = argon, and *C* = oxygen

It is worth pointing out that the definition of thermodynamic efficiency of Equation (1) is more accurate and reasonable than various other definitions[1,22] where minimum work of separation is directly compared to the total heat supplied to the reboiler, which implicitly assumes that this heat cannot be reused anywhere else once it gets removed by the condenser. This underlying assumption is clearly inaccurate for the applications listed above and for highly integrated plants where the rejected heat is often used elsewhere. In fact, the thermodynamic efficiency of distillation process calculated based on such definitions is usually abnormally small and can never reach 100% even for a fully reversible process,[23,24] which often leads to the misconception that distillation is always inefficient to operate compared to other separation processes such as membranes. The definition of Equation (1), however, captures the true thermodynamic efficiency of the distillation process itself.

The total work of separation in the denominator of Equation (1) is often explicitly expressed as the sum of minimum work of separation and *exergy loss* of the process:[15,16,25-27]

$$\text{total work of separation} = \text{minimum work of separation} + \text{exergy loss} \tag{2}$$

The exergy of a stream is equal to the maximum work obtainable when it is brought to the reference conditions via a reversible path.[28] To understand this, consider the schematic diagram of Figure 2, in which two equal quantities of heat duty Q_H (Q_C) at two different temperatures above (below) the reference point are brought to the reference condition using reversible heat engines (reversible heat pumps). Combining the first and the second law of thermodynamics, one can easily show that the work outputs from the reversible heat engines (heat pumps) are given by:

$$\begin{aligned} W_H &= Q_H\left(1-\frac{T_0}{T_H}\right) > W'_H = Q_H\left(1-\frac{T_0}{T'_H}\right) > 0 \\ W_C &= Q_C\left(1-\frac{T_0}{T_C}\right) < W'_C = Q_C\left(1-\frac{T_0}{T'_C}\right) < 0 \end{aligned} \tag{3}$$

in which a negative work output (i.e., W_C or W'_C) simply means that work input is required to "pump" the heat Q_C from a lower temperature level T_C or T'_C to the reference temperature T_0. From Equation (3), one can readily see that for the same amount of heat at different temperature levels, the one at more extreme temperature produces or requires more work (exergy) than the one at a milder temperature. Thus, we can determine the thermodynamic efficiency of the distillation process itself based on the exergy loss within the distillation column, which can be characterized by the temperature level at which the reboiler and condenser are operated.[16,17]

Agrawal and Herron[17] applied the concept of exergy analysis to determine the optimal thermodynamic efficiency of a distillation column separating ideal binary mixtures for several feed conditions and relative volatilities. Following the simplifying assumptions of ideal vapor–liquid equilibrium relations, constant relative volatilities, and constant and equal latent heats of vaporization for both components over the operating temperature range of the column, the authors made a groundbreaking discovery that *temperatures do not appear explicitly in the final efficiency expressions*.[17] Based on this finding, Agrawal and Herron[29] analyzed the optimal placement of an intermediate reboiler and/or intermediate condenser in a binary distillation column and derived several heuristics.[30] Although previous studies have been centered on binary mixture distillations, Agrawal and Fidkowski[23] also studied the thermodynamic efficiencies for conventional as well as "improved" direct and indirect split basic configurations for ternary mixture separations. As shown in Figure 3, the improved configurations modify the reboiler and condenser associated with interconnecting stream between the two distillation columns (also called submixture) to simultaneously produce two streams with the same composition, one as saturated liquid and the other as saturated vapor, that enter the next distillation column as feed. Using modified reboilers and condensers at submixtures locations reduces the total exergy loss of the distillation process.[23,31] Agrawal and Fidkowski[13] later extended their earlier idea[23] to analyze the thermodynamic efficiencies of ternary direct and indirect split thermally coupled configurations. However, since then, there have not been many attempts in the literature to further generalize this methodology to systematically account for distillation configurations that separate four or more components.

Because the size of regular-column configuration search space quickly explodes as the number of components in the feed increases,[5,32] it becomes too computationally expensive to possibly perform total exergy loss calculations for each configuration in the search space using process simulators such as Aspen Plus. One almost always needs to formulate an optimization problem that can be

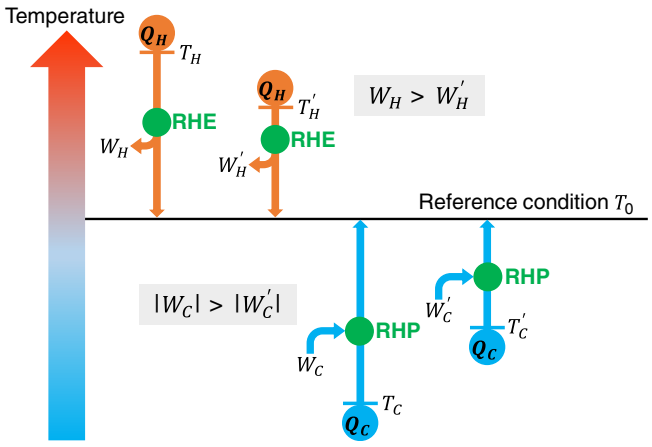

FIGURE 2 For the same amount of heat Q_H at two different temperature levels ($T_H > T'_H$) above the reference temperature T_0, the one at T_H generates more work W_H from the reversible heat engine (RHE) than the one at T'_H when both heats are brought to T_0 ($W_H > W'_H > 0$). Similarly, for the same amount of heat Q_C at T_C and T'_C ($T_C < T'_C$) which are lower than T_0, the one at the lower temperature T_C requires more work input from the reversible heat pump (RHP) than the one at T'_C when they are brought to T_0 ($W_C < W'_C < 0$) [Color figure can be viewed at wileyonlinelibrary.com]

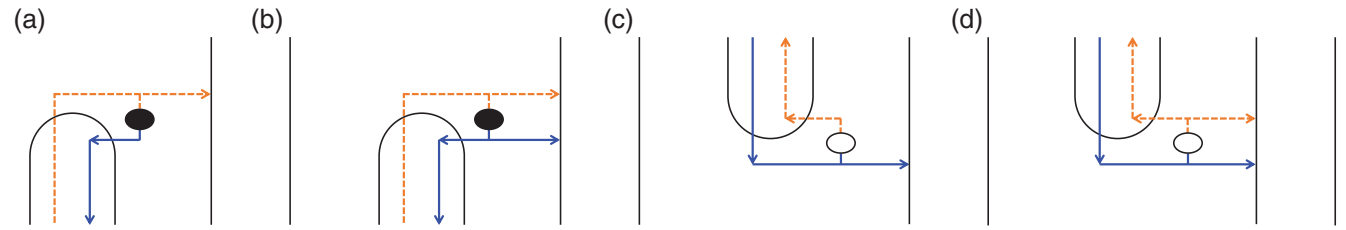

FIGURE 3 (a) A conventional submixture condenser; (b) modified condenser configuration generating two feed streams to the next column; (c) conventional submixture reboiler; (d) modified reboiler configuration producing two feed streams to the next column. Orange dashed lines indicate vapor flows and blue solid lines indicate liquid flows [Color figure can be viewed at wileyonlinelibrary.com]

quickly solved to explore the entire search space within a reasonable amount of time to identify one or a set of energy efficient configurations for a given separation task. The search for the global optimal configuration in the entire search space can be carried out using two distinct approaches. The first approach is to formulate the optimization problem as a single mixed-integer nonlinear programming (MINLP) problem.[9,33] If successful, this MINLP-based approach can find the global optimal solution without enumerating all the configurations in the search space. However, for many cases, the resulting MINLP could not be solved to global optimality due to various convergence difficulties.[33] Despite various attempts to tackle these issues, including proposing an alternative algorithm based on a modified version of logic-based outer-approximation algorithm[33] and decomposing the optimization problem into subproblems followed by introducing an iterative optimization procedure to solve them,[9] the MINLP-based approach still fails to guarantee global optimality.[34]

Besides the MINLP-based approach discussed above, a fundamentally different approach to search for the optimal distillation configuration is to first synthesize the complete search space, followed by formulating an optimization problem for each configuration in the search space. This is also known as the enumeration-based approach.[35] Recently, Nallasivam et al.[36] developed an enumeration-based global minimization algorithm (GMA) to minimize the total reboiler vapor duty requirement for each basic and thermally coupled regular-column configuration synthesized by the SA method.[5] In the GMA approach, the optimization for each configuration is formulated as a nonlinear programming problem (NLP) and can be solved to global optimality using a global solver, such as BARON[37] in a matter of seconds. A number of strategies, such as parallelization and bound tightening techniques,[36] can further bring down the computational time significantly. Later, Jiang et al.[34] extended the GMA framework and introduced an enumeration-based global optimization algorithm for determining the minimum cost of multicomponent distillation configurations. The objective of this article is to develop the first general global optimization algorithm that minimizes the total exergy loss (i.e., maximizes thermodynamic efficiency because the minimum work of separation in Equation (1) is a constant if feed and product specifications are known) for any regular-column distillation configuration. This NLP-based algorithm is referred to as the Global Minimization Algorithm for Exergy, or simply GMAE.

In the GMAE formulation, the majority of the GMA framework [36] is retained; additional exergy related relations and constraints are added as will be explained in the next section. Once the complete GMAE framework is introduced, we will examine a five-component case study involving recovery and fractionation of natural gas liquids (NGLs) to demonstrate the usefulness and robustness of the GMAE approach. By investigating several representative configurations in detail, we obtain physical insights behind how their construction translates into their performance and show how these insights can generate useful heuristics and guidelines for process engineers to identify energy efficient configurations. Next, several process intensification strategies will be considered to further improve the thermodynamic efficiency, eliminate equipment pieces, and save capital cost of a distillation configuration.

2 | NLP FORMULATION

Any optimization problem is described by the decision variables, the objective function, and the constraints. In the GMAE formulation, all the decision variables and constraints from the GMA framework are retained. The details of NLP formulation, along with the enumeration procedure and the bound tightening strategies, have thus been explicitly elucidated in Nallasivam et al.[36] In particular, we use the Underwood's method for minimum vapor duty calculations in each column section.[38] This implies that the GMAE model is constructed based on the same underlying assumptions as the GMA model, that is, ideal vapor–liquid equilibrium, constant relative volatility, as well as constant and equal latent heats for all components throughout the distillation columns.[36] Despite having to make these assumptions to simplify the model, it is found that the GMA approach still gives very accurate total reboiler duty estimates; this observation was made by comparing the results to those obtained by performing rigorous Aspen Plus simulations for zeotropic multicomponent separations using real thermodynamic models.[39]

Instead of using the total reboiler vapor duty requirement as in the GMA framework, the objective function for the GMAE is to minimize the total exergy loss $\Delta\varepsilon_{\text{loss}}$ for all distillation columns in a configuration. To formulate the $\Delta\varepsilon_{\text{loss}}$ expression of an arbitrary distillation configuration, we first consider an example configuration shown in Figure 4 involving four-component mixture separation. The

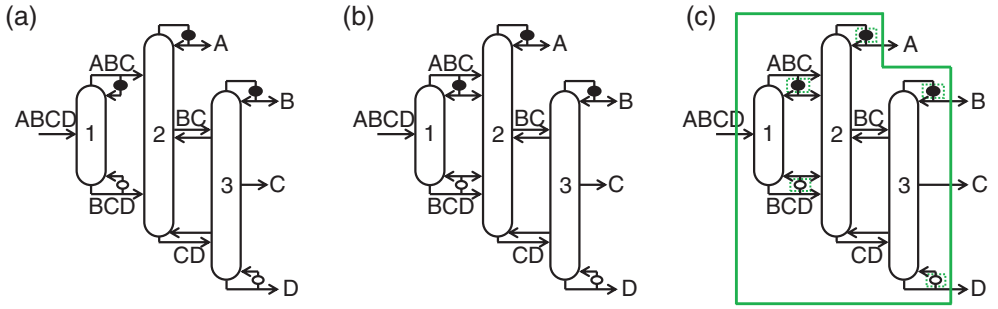

FIGURE 4 (a) An example configuration for four-component separation; (b) an improved configuration of (a) using modified reboiler at *BCD* and modified condenser at *ABC* following Figure 3; (c) the same configuration of (b) highlighting the control volume for exergy loss calculations. The control volume is defined as the large solid green box around the entire configuration followed by subtracting all the small regions enclosed by dashed green boxes around all reboilers and condensers to indicate that exergy losses associated with heat exchangers are excluded from the control volume [Color figure can be viewed at wileyonlinelibrary.com]

configuration of Figure 4a uses conventional heat exchangers at submixtures *ABC* and *BCD*, each producing one single-phase stream which then enters the next distillation column. However, the configuration of Figure 4b adopts the modified heat exchanger configurations at submixtures *ABC* and *BCD* following Figure 3 to simultaneously produce two streams with the same composition but different phases to enter the next column. In the GMAE model, users have the flexibility to specify either submixture heat exchanger scheme.

For illustration, let us examine the improved configuration of Figure 4b whose control volume for exergy loss calculation is explicitly drawn in Figure 4c. To calculate the total exergy loss of the distillation process alone for this configuration, only the exergy losses associated with material streams entering and leaving the distillation columns are considered. Exergy gains and losses of utility streams within the reboilers and condensers are excluded from the calculations. This is reflected in Figure 4c in which the dashed green boxes around all heat exchangers are subtracted from the region enclosed by the large green box around the configuration. Notice that the material streams entering and leaving the reboilers and condensers are still included in the control volume. The objective function is simply to minimize the total exergy loss of the distillation process $\Delta\varepsilon_{\text{loss}}$, which is the difference between the exergies associated with all material inflows and the exergies associated with all material outflows of the control volume:

$$\min\ \Delta\varepsilon_{\text{loss}} = \varepsilon_{ABCD} - \sum_{i=A}^{D}\varepsilon_i + \sum_{i\in\text{REB}}\left(\varepsilon_{i,\text{in}} - \varepsilon_{i,\text{out}}\right) + \sum_{i\in\text{COND}}\left(\varepsilon_{i,\text{in}} - \varepsilon_{i,\text{out}}\right), \quad (4)$$

in which ε_{ABCD} is the exergy of the main feed stream *ABCD*, and the sets REB and COND, respectively, store the indices of streams associated with reboilers and condensers, including the ones producing final pure products. In this example, REB = {*BCD*,*D*} and COND = {*ABC*,*A*,*B*}.

Each exergy term in the objective function of Equation (4) is contributed by the exergy associated with mixing (ε^M), thermal (ε^T), and pressure (ε^P) exergy associated with temperature and pressure change from the reference state to the saturated liquid state, as well as thermal exergy as a result of phase change (ε^ϕ). This means that $\varepsilon = \varepsilon^M + \varepsilon^P + \varepsilon^T + \varepsilon^\phi$. For pure components, $\varepsilon^M = 0$, and for any saturated liquid stream, including any final product stream which are taken at saturated liquid state as shown in Figure 4, $\varepsilon^\phi = 0$. When a material stream of one phase undergoes phase change inside a reboiler or condenser, the only contributor to the exergy difference is the thermal exergy associated with phase change. This exergy difference between a saturated liquid stream and a saturated vapor stream with the same composition, temperature, and pressure is given by:[28]

$$\begin{aligned}&\text{For pure component stream } i:\ \varepsilon_i^{\text{vap}} - \varepsilon_i^{\text{liq}} = F_i\Delta H\left(1 - \frac{T_0}{T_i}\right)\\ &\text{For mixture stream } i:\ \varepsilon_i^{\text{vap}} - \varepsilon_i^{\text{liq}} = F_i\Delta H\int_0^1\left(1 - \frac{T_0}{T_i}\right)dq,\end{aligned} \quad (5)$$

where ΔH is the molar latent heat of vaporization used to represent the multicomponent system (recall the constant and equal latent heat assumption for all components), F_i is the molar flow rate of material stream i, T_0 is the reference temperature, q stands for the thermal quality (liquid fraction) of the stream. Notice that integration is required when computing the exergy difference for a mixture stream i because its temperature T_i varies during phase change and is a function of the thermal quality q of the stream. However, for pure component streams, the expression simplifies because the temperature of the component remains constant during phase change.

Also, through extensive calculations for various mixtures, it is found numerically that the thermal or pressure exergy associated with a multicomponent mixture stream at its saturated liquid state is approximately equal to the sum of thermal or pressure exergies of the individual components at their saturated liquid states.[12,23] Combining this reasonable simplification with Equation (5) gives the exergy difference between the main feed stream *ABCD* with thermal quality of q_F and the sum of exergies of final product streams, that is, pure *A*, *B*, *C*, and *D* as shown in Figure 4c:

$$\varepsilon_{ABCD} - \sum_{i=A}^{D}\varepsilon_i = F_{ABCD}\left[RT_0\sum_{i=A}^{D}z_{i,F}\ln z_{i,F} + \Delta H\int_{q_F}^{1}\left[1 - \frac{T_0}{T_{ABCD}}\right]dq\right], \quad (6)$$

in which $F_{ABCD} = \sum_{i=A}^{D} F_i$ is the total molar flow rate of feed *ABCD*, *R* is the universal gas constant, and $z_{i,F} = F_i/F_{ABCD}$ is the net composition of component *i* in the main feed. The quantity $F_{ABCD}RT_0\sum_{i=A}^{D} z_{i,F}\ln z_{i,F}$ can be viewed as the exergy of a hypothetical mixture that has the same flow rate and composition as *ABCD* but is in saturated liquid state, subtracted by the sum of exergies of final pure products which are withdrawn as saturated liquid streams. The magnitude of this quantity exactly corresponds to the minimum work of separation in Equation (2) per unit time, which is also equal to the Gibbs free energy change of mixing for an ideal solution.[40] The integral term $F_{ABCD}\Delta H\int_{q_F}^{1}\left(1-\frac{T_0}{T_{ABCD}}\right)dq$ is instead derived from Equation (5) and is the exergy difference between the main feed stream *ABCD* and the hypothetical mixture. Substituting Equations (5) and (6) into (4) yields:

$$\begin{aligned}\Delta\varepsilon_{\text{loss}} &= F_{ABCD}RT_0\sum_{i=A}^{D} z_{i,F}\ln z_{i,F} + F_{ABCD}\Delta H\int_{q_F}^{1}\left(1-\frac{T_0}{T_{ABCD}}\right)dq \\ &+ \sum_{i\in\text{REB}} B_i\Delta H\int_0^1\left(1-\frac{T_0}{T_i}\right)dq - \sum_{i\in\text{COND}} D_i\Delta H\int_0^1\left(1-\frac{T_0}{T_i}\right)dq\end{aligned} \tag{7}$$

where B_i and D_i stand for the material flow rates that enter the reboiler and condenser associated with stream *i*, respectively.

Before simplifying Equation (7), we would like to introduce an alternative approach to derive the total exergy loss expression based on simple physical intuitions. From the control volume drawn in Figure 4c and Equation (3), one can easily see that the quantity $\sum_{i\in\text{REB}}\left(\varepsilon_{i,\text{in}}-\varepsilon_{i,\text{out}}\right)+\sum_{i\in\text{COND}}\left(\varepsilon_{i,\text{in}}-\varepsilon_{i,\text{out}}\right)$ in the objective function of Equation (4) is nothing but the excess total reversible heat pump work needed to condense and boil the streams after utilizing all the heat duties removed by the condensers to supply heat duties required by the reboilers in the configuration. This analogy between exergy loss and reversible heat pump work makes the derivation of Equation (7) easier and more intuitive. First, we may bring all the condenser duties to the reference temperature T_0 using reversible heat pumps. Notice that without loss of generality, we have assumed here that T_0 is higher than the boiling point of the heaviest component, T_D. From Figure 2 and Equation (3), the total reversible heat pump work input associated with condenser duties, denoted as HPW_{COND}, is simply:

$$\text{HPW}_{\text{COND}} = \sum_{i\in\text{COND}} D_i\Delta H\int_0^1\left(\frac{T_0}{T_i}-1\right)dq.$$

Of course, HPW_{COND} is more than what is needed to supply the reboiler duties at T_i, $i \in$ REB, which are all lower than T_0. Thus, in the next step, we need to determine the excess reversible heat pump work that needs to be subtracted from HPW_{COND} to obtain the true work requirement. And this excess work is simply the work input required to pump all the reboiler duties to T_0 reversibly:

$$\text{HPW}_{\text{REB}} = \sum_{i\in\text{REB}} B_i\Delta H\int_0^1\left(\frac{T_0}{T_i}-1\right)dq.$$

As a result, the true reversible heat pump work requirement, that is, the quantity $\sum_{i\in\text{REB}}\left(\varepsilon_{i,\text{in}}-\varepsilon_{i,\text{out}}\right)+\sum_{i\in\text{COND}}\left(\varepsilon_{i,\text{in}}-\varepsilon_{i,\text{out}}\right)$, is:

$$\begin{aligned}\text{HPW}_{\text{COND}} - \text{HPW}_{\text{REB}} &= \sum_{i\in\text{COND}} D_i\Delta H\int_0^1\left(\frac{T_0}{T_i}-1\right)dq \\ &- \sum_{i\in\text{REB}} B_i\Delta H\int_0^1\left(\frac{T_0}{T_i}-1\right)dq,\end{aligned}$$

which matches with the related terms in Equation (7) exactly.

Next, to simplify Equation (7), we follow the procedure of Agrawal and Herron[17,29,30] to perform an overall enthalpy balance on the control volume, which suggests that the sum of condenser duties must equal the sum of reboiler duties as well as the heat input required to vaporize a portion of the main feed stream to the specified thermal quality q_F:

$$\sum_{i\in\text{COND}} D_i\Delta H = \sum_{i\in\text{REB}} B_i\Delta H + (1-q_F)F_{ABCD}\Delta H,$$

which can also be expressed as:

$$\sum_{i\in\text{COND}} D_i\Delta H\int_0^1 dq = \sum_{i\in\text{REB}} B_i\Delta H\int_0^1 dq + F_{ABCD}\Delta H\int_{q_F}^{1} dq. \tag{8}$$

Now, multiplying both sides of Equation (8) with a constant factor $1-\frac{T_0}{T_D}$ and substituting the resulting expression into Equation (7) gives:

$$\begin{aligned}\Delta\varepsilon_{\text{loss}} &= F_{ABCD}RT_0\sum_{i=A}^{D} z_{i,F}\ln z_{i,F} - F_{ABCD}T_0\Delta H\int_{q_F}^{1}\left(\frac{1}{T_{ABCD}}-\frac{1}{T_D}\right)dq \\ &- T_0\sum_{i\in\text{REB}} B_i\Delta H\int_0^1\left(\frac{1}{T_i}-\frac{1}{T_D}\right)dq + T_0\sum_{i\in\text{COND}} D_i\Delta H\int_0^1\left(\frac{1}{T_i}-\frac{1}{T_D}\right)dq.\end{aligned} \tag{9}$$

Although the total exergy loss expression of Equation (9) does involve temperature, in the context of the GMAE model assumptions, the Clausius-Clapeyron relation actually implies that the need for temperature calculations can be completely eliminated.[17,41,42]

$$\begin{aligned}&\text{For pure component } i:\ \Delta H\left(\frac{1}{T_i}-\frac{1}{T_D}\right) = R\ln\alpha_i \\ &\text{For mixture stream } i:\ \Delta H\left(\frac{1}{T_i}-\frac{1}{T_D}\right) = R\ln\left(\sum_{j=A}^{D}\alpha_j x_{j,i}\right),\end{aligned} \tag{10}$$

where α_j is the relative volatility of component *j* with respect to the heaviest component *D*, and $x_{j,i}$ is the liquid mole fraction of component *j* in stream *i*. Note that in the derivation of Equation (10), pressure drops within the distillation system have been neglected. This simple but powerful result allows us to reformulate the objective function of Equation (9) for every distillation configuration by using only the decision variables introduced in the GMA framework. Substituting Equation (10) into Equation (9), the total exergy loss of the entire configuration of Figure 4c, normalized by a factor of RT_0,

can now be expressed using material stream composition variables alone:

$$\frac{\Delta\varepsilon_{\text{loss}}}{RT_0} = F_{ABCD}\sum_{i=A}^{D} z_{i,F}\ln z_{i,F} - F_{ABCD}\int_{q_F}^{1}\ln\left(\sum_{j=A}^{D}\alpha_j x_{j,ABCD}\right)dq - B_{BCD}\int_{0}^{1}\ln\left(\sum_{j=A}^{D}\alpha_j x_{j,BCD}\right)dq + D_{ABC}\int_{0}^{1}\ln\left(\sum_{j=A}^{D}\alpha_j x_{j,ABC}\right)dq + D_A\ln\alpha_A + D_B\ln\alpha_B \quad (11)$$

Observe that the above relation does not require explicit knowledge about any reboiler or condenser temperature![17,29,30]

Again, we remind the reader that $x_{j,i}$ in Equation (11), the liquid phase composition of component j in submixture stream i with a net material composition of $z_{j,i}$, is a function of thermal quality q which is governed by the phase equilibrium as:

$$z_{j,i} = qx_{j,i} + (1-q)\frac{\alpha_j x_{j,i}}{\sum_{k=A}^{D}\alpha_k x_{k,i}} \quad i\in\{ABC,\ BCD\} \quad (12)$$

To evaluate the integrals in Equation (11) numerically, we find that the two-point Gaussian quadrature method,[43] which approximates a definite integral of a function as a weighted sum of function values at two specific points, is sufficiently accurate for all practical cases that we have encountered. In other words, we replace each integral term in Equation (11) with the weighted sum of the integrand evaluated, by solving Equation (12), at two representative thermal quality values. Equation (12) is written out and solved at the two thermal quality values for every component, and the resulting set of solutions of liquid compositions can be substituted to evaluate the integrand to approximate the corresponding exergy loss term.

For higher accuracy, three-point or even higher Gaussian quadrature formula can be used. Nevertheless, as the number of weights used increases, the number of variables and nonconvexities also increase rapidly, unnecessarily making the GMAE formulation harder to solve to global optimality. In this case, there definitely exists a trade-off between numerical accuracy and the complexity of the problem, and an appropriate balance is needed. With this, the GMAE model formulation is now finalized. The NLP problem for each and every configuration synthesized by the SA method [5] is solved in GAMS using global solver BARON.[37] In the next section, we will examine an example involving shale gas separations in detail to illustrate the reliability and robustness of the GMAE framework as well as to generate some useful insights into the design and retrofit of energy efficient distillation configurations.

3 | CASE STUDY—NGL RECOVERY AND FRACTIONATION

The recent shale gas boom has transformed the energy landscape of the world, especially in the United States. Apart from methane and nitrogen, shale resources contain a substantial amount of natural gas liquids (NGLs), including ethane, propane, *n*-butane, *i*-butane, and other heavier hydrocarbons.[44] After acid gas removal and dehydration, the shale gas stream undergoes a series of separation steps using distillation to recover natural gas (mostly methane and a small amount of nitrogen) for storage or transport, as well as individual components of NGLs for downstream processing. In this study, we consider the NGLs' recovery and fractionation process for a typical shale gas stream produced from the Eagle Ford basin in Texas Shale Plays at a flow rate of 5,000 kmol/hr. Specifically, we consider the complete separation of five major components in the shale gas, namely natural gas (methane and nitrogen), ethane, propane, butane, and pentane (plus heavier hydrocarbons), which are respectively denoted as components *A*, *B*, *C*, *D*, and *E*. These pure components are finally produced as saturated liquid streams. After acid gas removal and dehydration, the shale gas is sent to the distillation trains as a saturated vapor feed. The molar composition of these five components in a typical shale gas stream in Eagle Ford can be found in He and You,[45] and the relative volatility information is obtained from Aspen Plus using Peng-Robinson equation of state model. These feed specifications are summarized in Table 1. The reference temperature T_0 is taken as the ambient temperature of 298 K.

In our enumeration based GMAE algorithm, a total of 6,128 independent NLP problems are automatically formulated in MATLAB for the corresponding 6,128 possible regular-column configurations generated from the five-component separation search space by the SA method.[5] Once formulated, each NLP problem is sent to GAMS via the GAMS/MATLAB interface [46] after which it is solved in GAMS using the BARON solver.[37] BARON intrinsically derives convex relaxations for standard bilinear and fractional nonlinear functions.[47] These convex relaxations are used by the solver to arrive at the global optimal solution. All 6,128 configurations are solved to global optimality (≤1% duality gap) within 4.54 hr of CPU time in a Dell OptiPlex 5040 desktop (Intel Core i7-6700 processor @ 3.40 GHz, 16 GB RAM, 64-bit Windows 7 OS) that simultaneously utilizes all four of its physical cores with the help of parfor functionality in MATLAB's Parallel Computing Toolbox.

Current industrial practices for NGLs' recovery and fractionation have been using the classic basic direct-split configuration drawn in Figure 5a. The GMAE determines that the minimum total exergy loss for this configuration is 5,775.46 MJ/hr (1.604 MW), and the corresponding reboiler vapor duty is 4,397.17 kmol/hr

TABLE 1 Feed specifications for a typical shale gas stream in Eagle Ford basin (reference: He and You[45])

Component	Mole fraction (%)	Relative volatility
Natural gas (*A*)	78.46	27.11
Ethane (*B*)	13.19	3.713
Propane (*C*)	5.27	1.579
Butane (*D*)	2.24	1.218
Pentane (*E*)	0.84	1

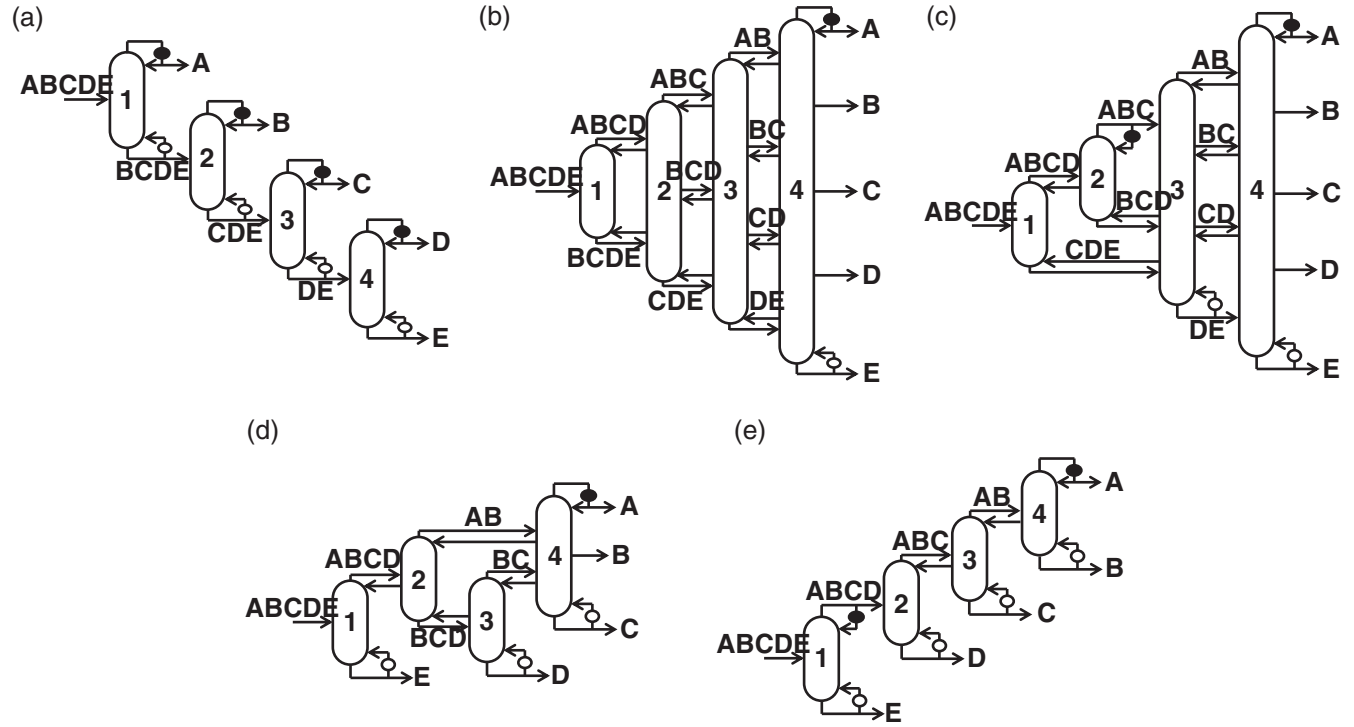

FIGURE 5 (a) Conventional basic direct-split configuration; (b) the fully thermally coupled (FTC) configuration; (c) the configuration with the lowest minimum total exergy loss among all configurations that require the same reboiler vapor duty as the FTC configuration; (d) the thermally coupled configuration that lies on the upper right corner of the linear upper bound of minimum total exergy loss versus reboiler vapor duty relationship; (e) a thermally coupled indirect split configuration which consumes almost the same reboiler vapor duty as (a) but has significantly more minimum total exergy loss

(1,221.4 mol/s). To compare the other 6,127 configurations in the search space with this "benchmark," we normalize the minimum total exergy losses of these configurations along with their corresponding total reboiler vapor duties, respectively, based on the values for the basic direct-split configuration. These results are shown in Figure 6. A number of interesting and important observations can be drawn from this plot. We will present some of these observations by discussing a few selected configurations that are highlighted in Figure 6 and are explicitly drawn in Figures 5 and 7.

First, we observe that the conventional basic direct-split configuration, which is represented by the red dot located at the lower right corner in Figure 6, is ranked 30th of all 6,128 configurations in the search space in terms of minimum total exergy loss (top 0.49%). Despite requiring a relatively high total reboiler duty as it involves all sharp split separations,[4] this conventional scheme is among the most thermodynamically efficient configurations. Meanwhile, another sharp-split configuration drawn in Figure 5e, which requires only about 0.4% more reboiler vapor duty than the conventional scheme, has >357.8% more minimum total exergy loss, making it the second worst configurations in the entire search space in terms of energy efficiency! In fact, Figure 6 shows no clear trend between a configuration's reboiler vapor duty and its thermodynamic efficiency. In general, a configuration with low reboiler vapor duty does not always correspond to a low total exergy loss. Likewise, a configuration that requires a high vapor duty may turn out to be quite efficient. This observation demonstrates the need for us to develop this GMAE algorithm to identify the most thermodynamically efficient configuration on top of the existing GMA algorithm [36] for minimizing total reboiler vapor duty.

To understand why these two configurations have drastically different minimum total exergy losses, recall from Table 1 that the natural gas stream (component *A*) is significantly more volatile compared to any other component in the system. Any condenser that produces a submixture containing the natural gas stream (i.e., associated with submixture *ABCD*, *ABC*, or *AB*) or produces the final natural gas product is operated at cryogenic temperature level considerably below ambient and thus requires an expensive cooling utility. Therefore, a small increase of cooling duty in any of these condensers will result in a significant increase in total exergy loss (utility cost) of the overall configuration. To improve the thermodynamic efficiency of the NGLs' recovery and fractionation process, it is critical to keep the condenser duties associated with streams containing the component *A* small.

For the conventional configuration of Figure 5a, the natural gas stream (*A*) is directly produced from column 1, whose condenser duty is given by 5,630.9 kmol/hr. However, in the configuration of Figure 5e, the sum of cooling duties at condensers *ABCD* (1,508.3 kmol/hr) and *A* (7,906.2 kmol/hr) increases to 9,414.5 kmol/hr, which leads to a significant increase in total exergy loss. It is worth noting that the condenser duty associated with the final natural gas product *A* increases by 40.4% compared to that in

the conventional configuration mainly because of the presence of thermal couplings at submixtures *ABC* and *AB*. Although introducing thermal couplings at these two submixtures might benefit the first-law heat duty, it really "hurts" the thermodynamic efficiency of the configuration. In this case, the basic configuration version for Figure 5e requires 7.3% more reboiler duty than the original thermally coupled configuration but has 13.5% less minimum total exergy loss. Thus, for applications in which the second-law temperature level penalty is more influential to the operating cost of a distillation configuration than the first-law heat duty benefit, thermal couplings of this sort should be avoided.[48]

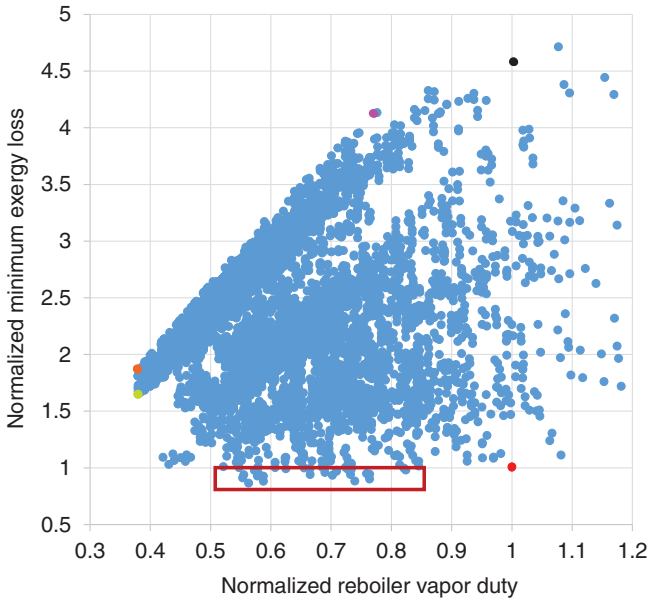

FIGURE 6 A plot showing the normalized minimum total exergy losses and the corresponding normalized total reboiler vapor duty requirements for all 6,128 configurations. Each dot represents a configuration. The red, green, orange, pink, and black dots in the plot are chosen as representatives and are drawn in Figure 5a through e, respectively. Potentially attractive configurations belonging to three major configuration families are also boxed. The representative configurations from each family are explicitly drawn in Figure 7 [Color figure can be viewed at wileyonlinelibrary.com]

The same reasoning can be used to analyze other representative configurations drawn in Figure 5 as well. For instance, the FTC configuration of Figure 5b is known to always have the lowest total reboiler vapor duty among all configurations in the search space.[49] Despite requiring 62.0% less vapor duty, the FTC configuration has 86.8% more minimum total exergy loss than the conventional configuration of Figure 5a, because all the vapor duty is generated at the highest temperature reboiler of *E* and condensed at the lowest temperature condenser at *A*. Fortunately, as we can see from Figure 6, there exist a total of 17 non-FTC configurations which have the same total vapor duty requirement as the FTC configuration but lower exergy loss. Among these 17 configurations, the one with the lowest minimum total exergy loss is drawn in Figure 5c. This configuration has two reboilers at *DE* and *E* as well as two condensers at *ABC* and *A*, thereby allowing the heat duty to be generated and removed by heat exchangers operated at milder temperature levels. These observations demonstrate that, for most industrial applications, building the FTC configuration is not a reasonable first choice.[12,50]

One interesting observation that one can make from Figure 6 is that, for a given total reboiler vapor duty value, there seems to be an upper bound on the minimum total exergy loss for a configuration. More interestingly, this upper bound seems to be linear with respect to the total reboiler vapor duty. We now discuss why such an upper bound is reasonable. Among all configurations that have the same reboiler vapor duty, the configuration with the highest minimum total exergy loss always corresponds to a completely thermally coupled (CTC) configuration in which all submixture heat exchangers are replaced with thermal couplings. The FTC configuration is a special CTC configuration. If submixture heat exchangers are eliminated, the heat duty is entirely generated and rejected by reboilers and condensers associated with final products, and such a change typically increases exergy loss. Unsurprisingly, the configurations that lie on the upper bound curve shown in Figure 6 are the CTC configurations with only one condenser at *A*. Final pure component products of intermediate relative volatilities (i.e., components *B*, *C*, and *D*) are either produced by reboilers or withdrawn from the distillation system as side-draw streams. It is easy to see why such CTC configurations have the lowest thermodynamic efficiencies among all configurations that require the same heat duty, as the only heat sink available in the entire configuration is at a temperature level significantly below the saturation

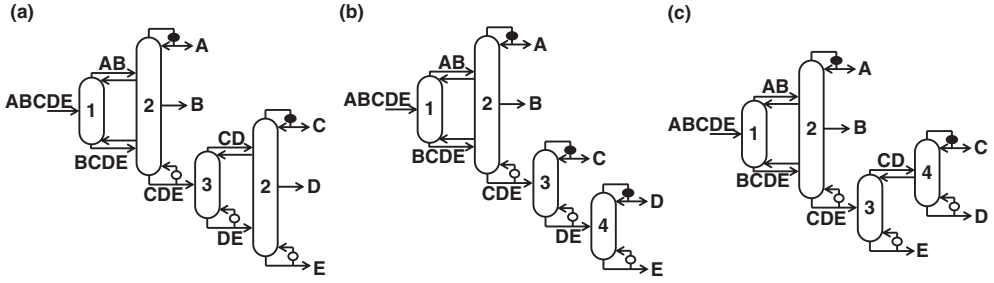

FIGURE 7 (a)–(c) The best performing configurations associated with each of the three configuration families highlighted in the box shown in Figure 6. The configurations of (a)–(c) are, respectively, ranked 1st, 3rd, and 20th among all 6,128 configurations in the search space in terms of minimum total exergy loss

temperature of the other streams. Because of the exergy loss expression of Equation (11), we expect the upper bound curve to be a linear function of total vapor duty generated at all reboilers as is the case in Figure 6.

As discussed, the FTC configuration is often located at the lower left endpoint of the upper bound line. We now consider the other endpoint, which corresponds to the configuration shown in Figure 5d. As we can see, all but one of the splits in this configuration are sharp splits, which suggests that this configuration has high vapor duty requirement. Thus, this CTC configuration is expected to result in a very high total exergy loss. We believe that this result applies to other multicomponent distillation problems as well. This observation can also be used as a heuristic to bound the objective function value from above in the optimization formulation and thus tighten the feasible region and expedite convergence to the global optimal solution. Note that one might expect the upper right endpoint of this upper bound line to correspond to the CTC version of the indirect split configuration of Figure 5e, as the configuration of Figure 5e has the highest minimum total exergy loss among all 6,128 configurations. However, this is not the case mainly because when a thermal coupling is introduced at *ABCD* in the configuration of Figure 5e, the total reboiler vapor duty reduces by 35.4% to 3,850.2 kmol/hr, thereby reducing the exergy loss at the condenser associated with the lightest component *A*. Just as for the submixture *ABCD* above, the GMAE framework allows process designers to identify useful thermal couplings that can reduce heat duty significantly while improving the thermodynamic efficiency of a given configuration.

Finally, we examine the best performing configurations identified by GMAE with respect to thermodynamic efficiency and categorize them into three distinct groups of configurations, where a representative for each group is shown in Figure 6. Configurations that belong to the same group carry out the same splits and are thus topologically indifferent; the only difference lies in the placements of their thermal couplings. The representative configuration drawn in Figure 7 was chosen as the best configuration within each group in terms of total exergy loss. When compared with the conventional basic direct-split scheme, configurations shown in Figure 7a through c reduce exergy loss by 13.4%, 11.6%, and 2.0% and require 43.7%, 26.1%, and 29.1% less total reboiler vapor duty, respectively. The exergy loss reduction for configuration of Figure 7a compared to the conventional scheme is further confirmed by performing meticulous sensitivity analysis on Aspen Plus using the RadFrac model and rigorous thermodynamic package. In fact, the configuration of Figure 7a is also the best performing configuration in terms of exergy loss among all 6,128 configurations in the entire search space. As we can see, the first two distillation columns in all three configurations of Figure 7 perform the same splits: one non-sharp split, $ABCDE \rightarrow AB/BCDE$, as well as two sharp splits, $AB \rightarrow A/B$ and $BCDE \rightarrow B/CDE$. The vapor duty needed for these three splits is either supplied by the saturated vapor feed stream or is generated by the reboiler *CDE*. The latter is 866.4 kmol/hr for each of the configurations in Figure 5. For the conventional configuration of Figure 5a, the sum of vapor duties generated by the two reboilers associated with *BCDE* and *CDE* is 2012.9 kmol/hr. By performing an enthalpy balance around columns 1 and 2, we find that, for the configurations in Figure 7, the sum of condenser duties for these two columns is 16.3% less than the corresponding sum for the conventional scheme. Thus, the best performing configurations reduce the sum of exergy losses associated with the first two distillation columns.

The total reboiler duties of the best configurations, which are highlighted with a box in Figure 6, span a wide range. This variation offers design engineers options in choosing the appropriate configuration to build or retrofit based on the actual mass and heat balances of the plant. These options are useful because although some of these configurations have much higher heat duties, they may be more attractive when one considers the heat integration opportunities with other process units. Also, configurations belonging to the group of configurations represented in Figure 7b are especially amenable for retrofitting, as two out of the four distillation columns in this group, namely columns 3 and 4, match those in the conventional configuration (see Figure 5a). Last but not least, as we show next, process intensification strategies such as dividing wall columns (DWCs) can be used to further reduce the size and capital cost of these configurations while maintaining their thermodynamic efficiencies.[50-52] Figure 8 shows one possible DWC implementation for each of the representative configurations drawn in Figure 7.[53] Note that three possible versions of DWC associated with the main feed stream are drawn in Figure 8. These DWC versions are completely thermodynamically equivalent to their corresponding configurations in Figure 7;[53] however, the ones shown in Figure 8b and c are fully operable in the sense that each zone separated by the vertical partition is associated with one reboiler or condenser so that the desired *L*/*V* ratio inside each zone can be achieved and precisely regulated.[54] Of course, more possible DWC versions that use 1 to 3 column shells can

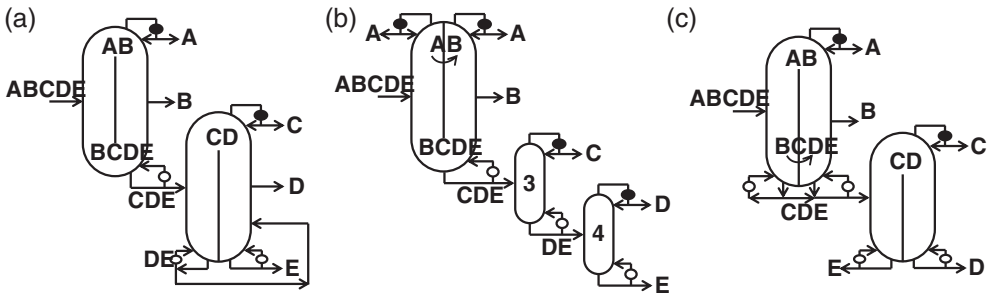

FIGURE 8 (a) One of the dividing wall column (DWC) versions of the configuration of Figure 7a; (b) a DWC version of the configuration of Figure 7b; (c) a DWC version of the configuration of Figure 7c

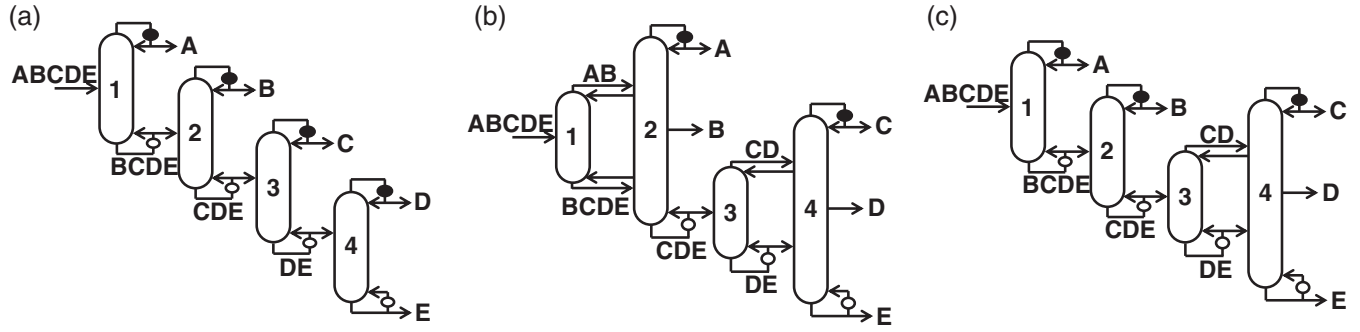

FIGURE 9 (a) Optimal retrofit design of the conventional scheme of Figure 5a using modified heat exchangers at submixtures. Notice that reboilers associated with submixtures *BCDE*, *CDE*, and *DE* now vaporizes all the bottoms liquid and produce vapor-only feed streams that enter the subsequent columns; (b) optimal retrofit design of the configuration of Figure 7a using modified heat exchangers at submixtures *CDE* and *DE*. This configuration also corresponds to the best performing configuration when using conventional submixture heat exchangers; (c) a new, attractive configuration design that ranked second among all 6,128 configurations in the new ranklist

be systematically synthesized for each of the regular-column configurations of Figure 7.[53]

4 | FURTHER IMPROVEMENT AND RETROFIT OPTIONS

In this section, we explore ways to further improve the heat duty and thermodynamic efficiency of an existing distillation system such as the conventional scheme of Figure 5a without having to change the topological structure of the configuration. In previous discussions, we have introduced the concept of using modified heat exchangers at submixture locations. We draw these modified designs for a submixture reboiler and a condenser in Figures 3b and d, respectively. These modified designs help improve the thermodynamic efficiency of a distillation configuration because they allow submixtures to have two phases.[23,31] In optimization parlance, the modified exchangers relax the feasible region of the formulation with only conventional heat exchangers. Thus, the thermodynamic efficiency of the best configuration with these designs is at least as high as that of any conventional configuration.

Our GMAE formulation is flexibly written so that users can easily enlarge the search space to admit these modified designs by simply relaxing the appropriate bounds on the liquid or vapor flow rate variables for the corresponding submixture streams. By enabling such modified designs, we obtain the new ranklist of distillation configurations in terms of their minimum total exergy losses. With this change, the ranking associated with the conventional configuration scheme moves up from 30th to 5th most thermodynamically efficient configuration. Figure 9a shows the optimal reboiler configurations at *BCDE*, *CDE*, and *DE*. This new reboiler arrangement reduces the minimum total exergy loss of the conventional scheme by 13.2% to 5,015.9 MJ/hr compared to original arrangement of Figure 5a, making it thermodynamically almost as efficient as the previously best performing configuration of Figure 7a. It is fascinating to see that substantial thermodynamic efficiency improvement can be achieved by simply modifying the submixture heat exchanger designs. Of course, in reality, to implement this new retrofit option, apart from modifying the related pipelines, valves, and fittings of the original configuration, the reboiler associated with submixture *BCDE* needs to be replaced to accommodate the large increase in its heat transfer area.

It turns out that, in the new ranklist obtained after implementing modified submixture heat exchangers, the configuration with the lowest minimum total exergy loss, which is drawn in Figure 9b, is also the optimal configuration (see Figure 7a) in the original ranklist except that it now uses modified designs for the heat exchangers. As reboilers of *CDE* and *DE* now vaporize all the bottoms liquid to produce vapor-only submixture streams, the minimum total exergy loss of this new design is 3.3% lower (4,834.6 MJ/hr) compared to that of the conventional heat exchanger arrangement in Figure 7a (4,999.8 MJ/hr).

It is also worth noting that the second best configuration in the new ranklist has a total exergy loss of 4,873.0 MJ/hr and is the configuration shown in Figure 9c. In this configuration, the first two distillation columns perform the same direct splits as in the conventional scheme of Figure 9a, whereas columns 3 and 4 resemble a prefractionator arrangement [19] except that submixture *CD* is associated with a thermal coupling.[55] As a result, columns 3 and 4 can be consolidated into a single dividing wall column, and this alternate arrangement can yield significant capital cost savings. In addition, compared to the improved version of the conventional scheme shown in Figure 9a, this new configuration of Figure 9c requires 17.3% less reboiler vapor duty, again suggesting that this configuration may have lower capital and operating costs. Moreover, when retrofitting the conventional configuration to this new configuration, the first two columns can be retained as they were, suggesting that this configuration may be attractive as a retrofit option.

Extending of the idea of modifying the submixture heat exchangers to produce two-phase feed streams, we can vaporize or condense a portion of the main feed stream before it enters the distillation system to further improve the thermodynamic efficiency of the overall process. This also opens up more opportunities for heat integration with other process units and utilities in the plant. This can be

done in the GMAE formulation by allowing the thermal quality q_F in the final objective function of Equation (11) to be a decision variable.

Last but not least, in the current GMAE formulation, all pure component streams are produced as saturated liquid products. However, depending on the actual problem, producing some or all of the final pure component products as saturated vapor or even two-phase streams may significantly improve the thermodynamic efficiency of a configuration further. Similar to preheating or precooling the feed, this new retrofit strategy can also be easily incorporated in the GMAE framework. In future publications, we will discuss in detail how the synergistic use of these strategies can help design more energy efficient multicomponent distillation systems.

5 | CONCLUSION AND FUTURE WORK

The operating cost of a distillation configuration depends not only on the first-law heat duty requirement but also on the temperature level at which heat duty is generated and rejected. The latter aspect, which is closely related to the thermodynamic efficiency of a distillation system, is often quantified by exergy analysis. We develop, for the first time, a GMAE that is based on the GMA framework by Nallasivam et al.[36] and minimizes the total exergy loss of any regular-column distillation configuration that can be used to distill any ideal or near-ideal multicomponent mixture and is synthesized by the SA method.[5] Using certain simplifying, yet reasonable, assumptions, we show that the final exergy loss expression does not require explicitly calculating the temperature. Instead, the only pieces of information required in exergy loss calculation are the readily available compositions of submixtures and the relative volatility of each component. The GMAE formulation is particularly useful for analyzing the operating cost of distillation systems where heat pumps are used and separations mainly driven by work rather than heat. In this article, we considered NGLs' recovery and fractionation process as an example to demonstrate the efficiency and usefulness of the GMAE framework. Through the discussion of this example, we derive several physical insights and observations regarding heat duty, thermodynamic efficiency, and exergy loss. In particular, a configuration with low heat duty does not always have high thermodynamic efficiency (e.g., the FTC or CTC configurations). However, a configuration that requires a high vapor duty may turn out to be quite thermodynamically efficient. The exergy loss is not distributed equally among the submixtures and final pure product streams. As a result, a small change in the reboiler or condenser duty associated with some of the critical streams can result in a significant change in the total exergy loss of the entire configuration. Moreover, replacing submixture heat exchangers with thermal couplings can have a similar effect. In particular, introduction of thermal couplings at certain submixture locations can reduce thermodynamic efficiency without providing any first-law heat-duty benefit. However, some thermal couplings can offer considerable heat duty savings without exhibiting any penalty in thermodynamic efficiency.[48] The GMAE thus provides industrial practitioners a quick and reliable screening tool to identify beneficial thermal coupling arrangements.

Once the screening phase using GMAE is complete and a handful of best performing configurations are identified, industrial practitioners can then perform detailed and rigorous process simulations on this small subset of configurations, which can now be done in much more manageable amount of time and effort. Finally, for the attractive, energy efficient distillation configuration identified by the GMAE and verified by process simulation, various process intensification strategies can be implemented, such as consolidating multiple distillation columns into a single-column shell in the form of dividing wall column, to further enhance the operability of the configuration, while also increasing its energy efficiency and reducing its size and capital cost. For an existing configuration, a simple retrofit option is identified which modifies heat exchangers at submixtures and improves thermodynamic efficiency and operational flexibility of the configuration. It is shown that this simple approach can significantly reduce the total exergy loss of a configuration without substantially increasing its capital expenditure.

Finally, we point out that the GMAE framework can be extended to consider more complex problems and other applications, including multi-effect distillation, heat-integrated distillation, and so on. For instance, although the total exergy loss characterizes the operating cost and energy efficiency of a distillation system that is work-driven, in practice, few multicomponent distillation systems are solely operated by either heat or work. Instead, for most multicomponent systems, especially those in which the boiling points of components cover a wide range (e.g., hydrocarbon separations from steam cracking), some distillation columns are operated by heat, whereas others are operated by work. In this case, a new objective function that models the true operating cost and/or energy efficiency of a distillation configuration is required. This new objective function must account for both the heat duty as well as the work input to the distillation column in a manner that accounts for the fact that, for the same magnitude, work input is more expensive than heat input. To do this, the current GMAE framework would have to be modified accordingly so that it can identify which form of energy is more suitable for driving each submixture or final product heat exchanger to minimize the combined heat and work input.

ACKNOWLEDGMENT

The information, data, or work presented herein was funded in part by the Office of Energy Efficiency and Renewable Energy (EERE), U.S. Department of Energy, under Award Number DE-EE0005768. The authors thank Radhakrishna Tumbalam Gooty and Tony Joseph Mathew for useful discussions.

ORCID

Rakesh Agrawal https://orcid.org/0000-0002-6746-9829

REFERENCES

1. Humphrey JL. Separation technologies: an opportunity for energy savings. *Chem Eng Prog*. 1992;88:32-42.
2. Shenvi AA, Shah VH, Zeller JA, Agrawal R. A synthesis method for multicomponent distillation sequences with fewer columns. *AIChE J*. 2012;58:2479-2494.
3. Agrawal R. Synthesis of multicomponent distillation column configurations. *AIChE J*. 2003;49(2):379-401.
4. Giridhar A, Agrawal R. Synthesis of distillation configurations: I. Characteristics of a good search space. *Comp Chem Eng*. 2010;34(1):73-83.
5. Shah VH, Agrawal R. A matrix method for multicomponent distillation sequences. *AIChE J*. 2010;56(7):1759-1775.
6. Thompson RW, King CJ. Systematic synthesis of separation schemes. *AIChE J*. 1972;18(5):941-948.
7. Sargent R, Gaminibandara K. Optimal design of plate distillation columns. In: Dixon L, ed. *Optimization in action*. New York: Academic Press; 1976.
8. Agrawal R. Synthesis of distillation column configurations for a multicomponent separation. *Ind Eng Chem Res*. 1996;35(4):1059-1071.
9. Caballero JA, Grossmann IE. Design of distillation sequences: from conventional to fully thermally coupled distillation systems. *Comp Chem Eng*. 2004;28(11):2307-2329.
10. Ivakpour J, Kasiri N. Synthesis of distillation column sequences for nonsharp separations. *Ind Eng Chem Res*. 2009;48(18):8635-8649.
11. Jiang Z, Madenoor Ramapriya G, Tawarmalani M, Agrawal R. Minimum energy of multicomponent distillation systems using minimum additional heat and mass integration sections. *AIChE J*. 2018;64(9):3410-3418.
12. Agrawal R, Fidkowski ZT. Are thermally coupled distillation columns always thermodynamically more efficient for ternary distillations? *Ind Eng Chem Res*. 1998;37(8):3444-3454.
13. Agrawal R, Fidkowski ZT. Thermodynamically efficient systems for ternary distillation. *Ind Eng Chem Res*. 1999;38(5):2065-2074.
14. Fonyó Z. Thermodynamic analysis of rectification - 1. Reversible model of rectification. *Int Chem Eng*. 1974;14:18-27.
15. Demirel Y. Thermodynamic analysis of separation systems. *Sep Sci Technol*. 2004;39(16):3897-3942.
16. Agrawal R, Woodward D. Efficient cryogenic nitrogen generators: an exergy analysis. *Gas Sep Purif*. 1991;5(3):139-150.
17. Agrawal R, Herron DM. Optimal thermodynamic feed conditions for distillation of ideal binary mixtures. *AIChE J*. 1997;43(11):2984-2996.
18. Seidel M. Verfahren zur Gleichzeitigen Zerlegung von Verflussigten Gasgemischen und anderen Flussigkeitsgemischen mit mehr als zwei Bestandteilen durch Rektifikation, German Patent 610503. 1935.
19. Petlyuk F, Platonov V, Slavinskii D. Thermodynamically optimal method for separating multicomponent mixtures. *Int Chem Eng*. 1965;5(3):555-561.
20. Agrawal R, Woodward D. Inter-column heat integration for multi-column distillation system. Washington, DC: U.S. Patent and Trademark Office. *US Patent 5230217*; 1993.
21. Flores OA, Crdenas JC, Hernndez S, Rico-Ramrez V. Thermodynamic analysis of thermally coupled distillation sequences. *Ind Eng Chem Res*. 2003;42(23):5940-5945.
22. Ho F, Keller G. *Process integration*. New York, NY: Wiley; 1987.
23. Agrawal R, Fidkowski ZT. Improved direct and indirect systems of columns for ternary distillation. *AIChE J*. 1998;44(4):823-830.
24. Cussler EL, Dutta BK. On separation efficiency. *AIChE J*. 2012;58(12):3825-3831.
25. Kaiser V, Gourlia L. The ideal column concept: applying exergy to distillation. *Chem Eng*. 1985;92(17):45-53.
26. Taprap R, Ishida M. Graphic exergy analysis of processes in distillation column by energy-utilization diagrams. *AIChE J*. 1996;42(6):1633-1641.
27. Fitzmorris RE, Mah RSH. Improving distillation column design using thermodynamic availability analysis. *AIChE J*. 1980;26(2):265-273.
28. Kotas T. *The exergy method of thermal plant analysis*. Stoneham, MA: Butterworth Publishers; 1985.
29. Agrawal R, Herron DM. Intermediate reboiler and condenser arrangement for binary distillation columns. *AIChE J*. 1998;44(6):1316-1324.
30. Agrawal R, Herron DM. Efficient use of an intermediate reboiler or condenser in a binary distillation. *AIChE J*. 1998;44(6):1303-1315.
31. Wankat PC, Kessler DP. Two-feed distillation. Same-composition feeds with different enthalpies. *Ind Eng Chem Res*. 1993;32(12):3061-3067.
32. Giridhar A, Agrawal R. Synthesis of distillation configurations. II: a search formulation for basic configurations. *Comp Chem Eng*. 2010;34(1):84-95.
33. Caballero JA, Grossmann IE. Generalized disjunctive programming model for the optimal synthesis of thermally linked distillation columns. *Ind Eng Chem Res*. 2001;40(10):2260-2274.
34. Jiang Z, Mathew TJ, Zhang H, et al. Global optimization of multicomponent distillation configurations: global minimization of total cost for multicomponent mixture separations. *Comp Chem Eng*. 2019;126:249-262.
35. Nallasivam U, Shah VH, Shenvi AA, Tawarmalani M, Agrawal R. Global optimization of multicomponent distillation configurations: 1. Need for a reliable global optimization algorithm. *AIChE J*. 2013;59(3):971-981.
36. Nallasivam U, Shah VH, Shenvi AA, Huff J, Tawarmalani M, Agrawal R. Global optimization of multicomponent distillation configurations: 2. Enumeration based global minimization algorithm. *AIChE J*. 2016;62(6):2071-2086.
37. Tawarmalani M, Sahinidis NV. A polyhedral branch-and-cut approach to global optimization. *Math Prog*. 2005;103:225-249.
38. Underwood A. Fractional distillation of multicomponent mixtures. *Chem Eng Prog*. 1948;44:603-614.
39. Madenoor Ramapriya G, Selvarajah A, Jimenez Cucaita LE, Huff J, Tawarmalani M, Agrawal R. Short-cut methods versus rigorous methods for performance-evaluation of distillation configurations. *Ind Eng Chem Res*. 2018;57(22):7726-7731.
40. Sandler SI. *Chemical, biochemical, and engineering thermodynamics*. 4th ed. Hoboken, N.J.: John Wiley; 2006.
41. Glinos K, Malone MF, Douglas JM. Shortcut evaluation of ΔT and QΔT for the synthesis of heat integrated distillation sequences. *AIChE J*. 1985;31(6):1039-1040.
42. Glinos K, Malone M. Net work consumption in distillation – short-cut evaluation and applications to synthesis. *Comp Chem Eng*. 1989;13(3):295-305.

43. Chapra SC. *Numerical methods for engineers*. 7th ed. New York, NY: McGraw-Hill Higher Education; 2015.
44. Bullin KA, Krouskop PE. Compositional variety complicates processing plans for US shale gas. *Oil Gas J*. 2009;101(10):50-55.
45. He C, You F. Shale gas processing integrated with ethylene production: novel process designs, exergy analysis, and techno-economic analysis. *Ind Eng Chem Res*. 2014;53(28):11442-11459.
46. Ferris MC, Dirkse S, Ramakrishnan J. MATLAB and GAMS: Interfacing Optimization and Visualization Software (the GDXMRW utilities). 2011. http://research.cs.wisc.edu/math-prog/matlab.html
47. Tawarmalani M, Sahinidis NV. *Convexification and global optimization in continuous and mixed-integer nonlinear programming: theory, algorithms, software, and applications*. Boston: Kluwer Academic Publishers; 2002.
48. Shah VH, Agrawal R. Are all thermal coupling links between multicomponent distillation columns useful from an energy perspective? *Ind Eng Chem Res*. 2011;50(3):1770-1777.
49. Halvorsen IJ, Skogestad S. Minimum energy consumption in multicomponent distillation. 3. More than three products and generalized Petlyuk arrangements. *Ind Eng Chem Res*. 2003;42(3):616-629.
50. Jiang Z, Agrawal R. Process intensification in multicomponent distillation: a review of recent advancements. *Chem Eng Res Des*. 2019;147:122-145.
51. Schultz MA, Stewart DG, Harris JM, Rosenblum SP, Shakur MS, O'Brien DE. Reduce costs with dividing-wall columns. *Chem Eng Prog*. 2002;98(5):64-71.
52. Jiang Z, Madenoor Ramapriya G, Tawarmalani M, Agrawal R. Process intensification in multicomponent distillation. *Chem Eng Trans*. 2018;69:841-846.
53. Madenoor Ramapriya G, Tawarmalani M, Agrawal R. A systematic method to synthesize all dividing wall columns for n-component separation: part I. *AIChE J*. 2018;64(2):649-659.
54. Madenoor Ramapriya G, Tawarmalani M, Agrawal R. A systematic method to synthesize all dividing wall columns for n-component separation: part II. *AIChE J*. 2018;64(2):660-672.
55. Agrawal R, Fidkowski ZT. New thermally coupled schemes for ternary distillation. *AIChE J*. 1999;45(3):485-496.

How to cite this article: Jiang Z, Chen Z, Huff J, Shenvi AA, Tawarmalani M, Agrawal R. Global minimization of total exergy loss of multicomponent distillation configurations. *AIChE J*. 2019;65:e16737. https://doi.org/10.1002/aic.16737